

Transcription Factor VAX1 Regulates the Regional Specification of the Subpallium through Repressing *Gsx2*

Yan Wen

Fudan University

Zihao Su

Fudan University

Ziwu Wang

Fudan University

Lin Yang

Fudan University

Guoping Liu

Fudan University

Zicong Shang

Fudan University

Yangyang Duan

Fudan University

Heng Du

Fudan University

Zhenmeiyu Li

Fudan University

Yan You

Fudan University

Xiaosu Li

Fudan University

Zhengang Yang

Fudan University

Zhuangzhi Zhang (✉ zz_zhang@fudan.edu.cn)

Fudan University <https://orcid.org/0000-0002-9860-6689>

Research

Keywords: Vax1, Gsx2, subpallium, development, telencephalon

Posted Date: December 14th, 2020

DOI: <https://doi.org/10.21203/rs.3.rs-113451/v2>

License:  This work is licensed under a Creative Commons Attribution 4.0 International License.

[Read Full License](#)

Version of Record: A version of this preprint was published at Molecular Neurobiology on April 5th, 2021.

See the published version at <https://doi.org/10.1007/s12035-021-02378-x>.

Abstract

Specification of the progenitors' regional identity is a pivotal step during development of the cerebral cortex and basal ganglia. The molecular mechanisms underlying progenitor regionalization, however, are poorly understood. Here we showed that the transcription factors *Vax1* was highly expressed in the developing subpallium. In its absence, the RNA-Seq analysis, in situ RNA hybridization, and immunofluorescence staining results showed that the cell proliferation was increased in the subpallium, but the neuronal differentiation was blocked. Moreover, the dLGE region severely expanded ventrally at the expense of the vLGE, MGE, and septum. Finally, overexpressed VAX1 in the LGE progenitors strongly inhibits *Gsx2* expression. Taken together, our findings show that *Vax1* is crucial for subpallium regionalization by repressing *Gsx2*.

1 Introduction

The telencephalon originates from the rostral nerve plate. During development, the telencephalon acquires precise subdivisions both along the dorsal-ventral (DV) and the anteroposterior (AP) axis [1-3]. The telencephalon is subdivided into two different territories: pallium and subpallium. The subpallium consists of the lateral ganglionic eminence (LGE), medial ganglionic eminence (MGE), caudal ganglionic eminence (CGE), preoptic area (POA), and septum. The progenitors located in different regions generate different cell types during telencephalic development. For example, the progenitors in the dLGE give rise to the olfactory bulb (OB) interneurons. In contrast, the progenitors in the vLGE mainly contribute to striatal medium-sized spiny neurons (MSNs) [4-6]. Thus, the maintenance of the dLGE, vLGE, MGE, and POA region in the subpallium is crucial for telencephalon development.

Multiple signaling pathways and transcription factors are involved in regionalization of the telencephalon. In the early embryonic stage, *Fgf8* and *Shh* signaling are required for telencephalon patterning. Deletion of *Fgf8* leads to structural abnormalities of the dorsal and ventral telencephalon [7, 8]. In *Shh*^{-/-} mouse embryos, all ventral telencephalic progenitors are missing as detected by loss of ventral markers including *Gsx2*, *Nkx2.1*, and *Dlx2* [9, 10]. In the subpallidum development, several genes have been found responsible for regionalization. Transcription factors *Gsx2* and *Pax6* play complementary roles in dorsal-ventral patterning of the telencephalon [11]. A ventral to dorsal transformation leads the pallidal primordium into a striatal-like anlage in the *Nkx2.1* knock out mice [12, 13]. *Otx2* also plays crucial roles in MGE patterning through specifying vMGE fate and repressing POA fate [14]. The mechanisms of activation and mutual repression of the transcription factors in progenitors to establish regional patterning, however, need to be further investigated. For example, the key transcription factor, *Gsx2*, is not only required for the generation of the striatal MSNs and OB interneurons but is also crucial for the regionalization of the PSB (pallial-subpallial boundary) during forebrain development [4, 11, 15, 16]. The exact mechanism of down-regulating its expression in the vLGE/MGE, however, is largely unknown.

The homeobox transcription factor *Vax1* starts to express at approximately embryonic day (E) 8 in mice. *Vax1-mRNA* is detected in the most rostral level of the medial neural plate at E8. As development proceeds, *Vax1* is found in the basal forebrain, optic stalk, optic disk, and medial olfactory placode [17]. Previous studies showed that secreted VAX1 protein regulates retinal axon growth and is required for axon guidance and major tract formation [18]. *Vax1* is also required for the precursor cells proliferating in the SVZ and migrating through the rostral migratory stream (RMS) to the OB [19]. In addition, this generation of cortical interneurons is compromised in the *Vax1*^{-/-} mice [20]. Recently, studies showed that regulatory interactions between *Vax1* and *Pax6* are crucial for stem cell regionalization during olfactory bulb neurogenesis [21]. Finally, heterozygous deletion of *Vax1* gene causes subfertility in mice and variants in *VAX1* genes are associated with non-syndromic cleft lip in humans [22, 23]. Although *Vax1* plays important roles in subpallium development, the mechanisms of *Vax1* in regulating subpallium regionalization remain largely unknown.

Here, our results show that *Vax1* is crucial for the regionalization of the subpallium. In the *Vax1* mutants, the dLGE expands ventrally, the vLGE and MGE get smaller, and the septum is absent. Furthermore, we found that the expression of *Gsx2* in the vLGE and MGE was significantly increased. Lastly, ectopic overexpression of *Vax1* leads to a significant decrease the expression of *Gsx2* in the LGE. Thus, *Vax1* may regulate subpallium regionalization by repressing *Gsx2*.

2 Materials And Methods

2.1 Mice

All experiments conducted in this research study were in accordance with guidelines from Fudan University. *Vax1*^{tm1b(KOMP)MBP} (*Vax1*^{+/-}) mice were obtained from The Jackson Laboratory (Bar Harbor, Maine). *Vax1*^{-/-} mice were obtained from crossing *Vax1*^{+/-} with *Vax1*^{+/-} mice. All mice were maintained in a mixed genetic background of C57BL/6J and CD1. Noon of the day of vaginal plug detection was considered as E0.5 and the day of birth was defined as P0.

Genotyping of *Vax1*^{-/-} mice by PCR using the following primers:

Vax1-WT-F: CCAAGGGGGCTAACTTCATAC

Vax1-WT-R: CTCCTCCTTCTGCTGTCTGG

Vax1-Mut-F: CGGTCGCTACCATTACCAGT

Vax1-Mut-R: AAGCCCTGGTTTCTCTGACA

2.2 BrdU Labeling

A single intraperitoneal injection of 50 mg/kg BrdU was administered at E16.5. BrdU incorporation was analyzed 30 minutes after BrdU injection.

2.3 Tissue Preparation

Tissue preparation was performed as previously described [24].

2.4 Immunofluorescence

Immunofluorescence staining was performed as previously described [25].

The primary antibodies used in this study were as follows:

- (1) Rabbit anti-GSX2 (Millipore Cat#ABN162, RRID: AB_11203296, Dilutions 1:2000)
- (2) Goat anti-SP8 (Santa Cruz Biotechnology Cat# sc-104661, RRID: AB_2194626, Dilutions 1:1000).
- (3) Rat anti-BrdU (Accurate Chemical and Scientific Corporation Cat# OBT0030S, Dilutions 1:200).
- (4) Rabbit anti-FOXP1 (Abcam Cat# ab16645, Dilutions 1:2000).
- (5) Rabbit anti-Ki67 (Vector Labs, Cat# VP-K451, Dilutions 1:500).
- (6) Chicken anti-GFP (Aves Labs, Cat# GFP-1020, Dilutions 1:2000).

All secondary antibodies used in this study were from Jackson ImmunoResearch Labs.

Secondary Antibodies	Cat Number
Alexa®488-conjugated Affinipure Donkey Anti-Rabbit IgG (H ⁺ L)	711-545-152
Cy TM 3-conjugated Affinipure Donkey Anti-Rabbit IgG (H ⁺ L)	711-165-152
Alexa®488-conjugated Affinipure Donkey Anti-Mouse IgG (H ⁺ L)	715-545-151
Cy TM 3-conjugated Affinipure Donkey Anti-Mouse IgG (H ⁺ L)	715-165-151
Alexa®488-conjugated Affinipure Donkey Anti-Chicken IgY ⁺⁺ (IgG) (H ⁺ L)	703-545-155
Cy TM 3-AffiniPure Donkey Anti-Chicken IgY (IgG) (H ⁺ L)	703-165-155
Alexa®488-conjugated Affinipure Donkey Anti-Goat ⁺⁺ (IgG) (H ⁺ L)	705-545-147
Cy TM 3-AffiniPure Donkey Anti-Goat IgG (H ⁺ L)	705-505-147
Cy TM 3-AffiniPure Donkey Anti-Rat IgG (H ⁺ L)	712-165-150
Cy TM 3-AffiniPure Donkey Anti-Guinea Pig IgG (H ⁺ L)	706-165-148

2.5 In Situ RNA Hybridization

In situ hybridization was performed on 20 μm thick cryo-sections using digoxigenin riboprobes, as previously described [26]. Probes were made from P0 wild type mouse brain cDNA amplified by PCR using the following primers

<i>Vax1</i>	F: TCCTGTCTAGAACAGAGCTGATGGG R: CTGTGGTTTTGGTTAAATTGCGAG
<i>Gsx2</i>	F: CCTTTGTTTCGAGTCCCAGACACC R: AAAGGGACTTCCAGAGACCTGGAT
<i>Etv1</i>	F: TTCATGGCCTCCCACTGAAAATC R: CCTTCGTTGTAGGGGTGAGGGTT
<i>Tshz1</i>	F: GAGAAGGTCACGGGCAAGGTCAGC R: GAGGCGAGGACACAGCATCTGCCA
<i>Prokr2</i>	F: ATGGGACCCCAGAACAGA R: ATAGATACGCTACTTCAAAGATGAG
<i>Isl1</i>	F: ATGGGAGACATGGGCGATCC R: CATGCCTCAATAGGACTGGCTACC
<i>Drd1</i>	F: ATGGCTCCTAACACTTCTACCATGG R: TCAGGTTGAATGCTGTCCGCTGTG
<i>Drd2</i>	F: CGGGAGCTGGAAGCCTCGA R: TGCAGGGTCAAGAGAAGGCCG
<i>Lhx6</i>	F: CAGAGAGGGCGCGCATGGTCACCT R: AATTGGGGGGGGGGTCTTTGGCAC
<i>Lhx8</i>	F: GCCTTAGTGTGGCTGAGAGA R: AGGATGGTAGGCTTTGTAAACT
<i>Nkx2.1</i>	F: TCCTAGTCAAAGACGGCAAACCCT R: TAAAGAGAAAGGAAGGGGGGAAAGA
<i>Gbx1</i>	F: GATGAAGAGAAGCTAGAGCCCCCA R: GGTTTCAGATCCTGTGACTTCCGGT
<i>Gbx2</i>	F: GTTCGCTATTTCGAAGTCAACACCAG R: AATTAAACACAACGGAGACGTGCTT
<i>Cdca7</i>	F: AGACTCTCGAGACGTTTGCTA R: AGCTGCAGTTGCAAATTCCTC
<i>Ccnd2</i>	F: GGGCTAGCAGATGACGAACACG

	R: TCCCATTCAGCCAAAGGAAGGA
<i>Ascl1</i>	F: CTAACAGGCAGGGCTGGA
	R: TAAGGGGTGGGTGTGAGG
<i>Dlx1</i>	F: ATGACCATGACCACCATGCCAG
	R: TCACATCAGTTGAGGCTGCTGC
<i>Dlx2</i>	F: TTTCTGTCCCGGGTCAGGAT
	R: AAGTCTCAGACGCTGTCCACTCGA
<i>Dlx5</i>	F: CAGCTTTCAGCTGGCCGCTT
	R: CAAGGCACCATTGATAGTGTCCACA
<i>LacZ</i>	F: CTCTATCGTGCGGTGGTTGAACT
	R: GGGTTGCCGTTTTTCATCATATTT

2.6 RNA-Seq

RNA sequencing (RNA-Seq) analysis was performed as previously described [26]. The ganglionic eminence from the E13.5 *Vax1*^{-/-} and littermate *WT*, and lateral ganglionic eminence from the E16.5 *Vax1*^{-/-} and littermate *WT* were dissected (n=3). Gene expression levels were reported in FPKM (fragments per kilobase of exon per million fragments mapped).

2.7 Cloning of the pCAG-*Vax1*-ires-GFP expression plasmid and in vivo electroporation

The *Vax1* CDS was cloned from *WT* P0 cDNA amplified by PCR using the following primers: F- ATGTTTCGGGAAACCAGACAAAATGG; R-AAATCAGTCCAGCGCTTTTTTCTCG. It was then inserted into the pCAGGS-ires-EGFP vector, using XbaI and EcoRI restriction sites. DNA-sequencing was performed to make sure no mutation was generated during the cloning. In vivo electroporation was performed at P0. Plasmids pCAG-GFP (Addgene #11150) or pCAG-*Vax1*-ires-GFP, (final concentration of 1-2 mg/ml, 1µl each embryo), were mixed with 0.05% Fast Green (Sigma), and injected into the lateral ventricle using a beveled pulled glass micropipette. Five electrical pulses (duration: 50 ms) were applied at 130V across the uterine wall with a 950 ms interval between pulses. Electroporation was performed using a pair of 7 mm platinum electrodes (BTX, Tweezertrode 45-0488, Harvard Apparatus) connected to an electroporator (BTX, ECM830). Pups were analyzed at P3.

2.8 Quantification

The numbers of BrdU and *Foxp1* positive cells in the LGE SVZ were quantified in 9 randomly chosen 20 µm sections from each mouse. Three control and *Vax1* mutant mice from each group were analyzed at

E16.5. The integrated density of *Cdca7*, *Ccnd2*, *Ascl1*, *Dlx1*, *Dlx2*, *Dlx5* and *Isl1* measured by Image J in the LGE SVZ were quantified in 9 randomly chosen 20 μm sections from each mouse. Three control and *Vax1* mutant mice from each group were analyzed at E16.5. For quantification of GFP⁺ and GFP⁺/GSX2⁺ cells in the mouse lateral ventricular zone at P3. Images were collected with an Olympus VS 120 microscope using a 20X objective. Six 20- μm thick coronal sections from rostral, intermediate, and caudal levels of the striatum were selected (n=5 mice per group). We selected the dorsal-most lateral ventricular VZ/SVZ region (1500 pix X 1500 pix) to quantify the number of GFP⁺ and GFP⁺/GSX2⁺ cells in each group.

2.9 Microscopy

Figures were imaged with an Olympus VS 120 microscope. Images were merged, cropped, and optimized in Adobe Photoshop CC without distorting the original information.

3 Results

3.1 Increase of cell proliferation in the *Vax1*^{-/-} subpallium V-SVZ

The Ventral Homeodomain Protein 1 (VAX1) is highly expressed in the subpallium progenitors from embryonic day 12.5 (E12.5) to adult would suggest *Vax1* plays an important role in forebrain development (See Supplementary fig. S1a-f, Additional File 1). To investigate whether *Vax1* regulates cell proliferation, we first performed 30-min BrdU pulse labeling at E16.5 and BrdU immunofluorescence staining. The number of BrdU⁺ cells in the *Vax1*^{-/-} LGE gradually increased in a rostral to caudal pattern, compared to controls (Fig. 1a-c', j). This means the number of cells in S-phase of the cell cycle was increased after *Vax1* deletion. Since *Cdca7* is a cell division cycle associated gene and *Ccnd2* promotes cell cycle progression from G1 to S phase, we then checked these genes at E16.5. In situ RNA hybridization of *Cdca7* and *Ccnd2* showed that *Cdca7-mRNA*⁺ and *Ccnd2-mRNA*⁺ cells were also significantly increased (Fig. 1d-i', k, l). The above results illustrated that there is an increase of cell proliferation in the *Vax1*^{-/-} subpallium. This is consistent with previous *in vitro* neurosphere culture results [19].

3.2 *Vax1* promotes neuronal differentiation in the subpallium V-SVZ

The bHLH transcription factor, *Ascl1*, is heavily expressed in ventral forebrain progenitors, and *Ascl1* is crucial for neurogenesis [27]. At E16.5, the number of *Ascl1*⁺ cells in the *Vax1*^{-/-} subpallium VZ (ventricular zone) was significantly increased, compared to controls (Fig. 2a-c', m). *Dlx1* and *Dlx2* are mainly expressed in the VZ and SVZ of the subpallium, *Dlx5* appears later than *Dlx1/2*, and is expressed in more differentiated neurons in the SVZ (subventricular zone) and MZ (mantle zone). Our results showed that *Dlx1*⁺, *Dlx2*⁺ and *Dlx5*⁺ cells in the *Vax1*^{-/-} subpallium were increased markedly (Fig. 2d-l', m). Accumulation of *Ascl1*⁺, *Dlx1*⁺, *Dlx2*⁺ and *Dlx5*⁺ immature neurons in the *Vax1*^{-/-} VZ and SVZ suggests

that neural progenitors in the subpallium could not normally exit the cycle and differentiate. Therefore, *Vax1* promotes neuronal differentiation in the subpallium VZ-SVZ.

3.3 The expansion of the dLGE domain in the *Vax1*^{-/-} mice

The progenitors in the dLGE mainly give rise to olfactory bulb interneurons. Strong expression of *Gsx2* in the dLGE promotes the activation and lineage progression of OB interneuron progenitors. *Sp8* is expressed in migrating neuroblasts in the embryonic dLGE, postnatal SVZ and most OB interneurons, and the OB interneuron defects in conditional inactivation of *Sp8* mice [6]. *Sp8* regulates the expression of *Tshz1* and *Prokr2* [28]. *Prokr2* and *Tshz1* are expressed in the SVZ-RMS-OB, severe tangential, and radial migration defects of neuroblasts in *Prokr2-KO* mice [24, 29]. *Etv1*⁺ cells in the dLGE and postnatal SVZ travel through the RMS into the OB where they mature into OB interneurons. At E16.5, we found that these dLGE markers (*Gsx2*, *Etv1*, *Sp8*, *Tshz1* and *Prokr2*) were significantly increased in the *Vax1*^{-/-} mice (Fig. 3a-o'). *Gsx2* was heavily expressed in progenitors of the dLGE and its expression showed a ventral-low to dorsal-high gradient in the subpallium of the controls whereas, more GSX2⁺ cells were seen in the VZ/SVZ of the vLGE and MGE. The obvious ventral to dorsal gradient in GSX2⁺ cell numbers in the *Vax1*^{-/-} mice disappeared (Fig. 3a-c'). Even more remarkably, *Prokr2*, *Tshz1*, *Etv1*, and *Sp8* showed an increased gradient expression in the dLGE (Fig. 3d-o'). *Gsx2* is expressed in proliferating progenitors, *Sp8* is found in some dividing cells, and *Prokr2* is observed in post-mitotic immature interneurons, suggesting the blockage of neuronal differentiation in the dLGE after *Vax1* gene deletion. The expression of these markers (*Gsx2*, *Sp8* and *Prokr2*) was also significantly increased in the *Vax1*^{-/-} mice at P0 (data not shown). Taken together, the progenitors and immature neurons in the dLGE are significantly increased in the *Vax1*^{-/-} mice.

3.4 The vLGE derived striatal MSNs were reduced in *Vax1* mutant mice

We showed above that the dLGE was expanded, next we wanted to know whether the vLGE and MGE-derived neurons changed or not. *Isl1* was highly expressed in D1-type MSNs [30, 31]. At E16.5, *Isl1*⁺ cells were significantly reduced in the LGE SVZ and MZ of the *Vax1*^{-/-} mice (Fig. 4a-c', m). More than 90% striatal MSNs are expressed *Foxp1*. The number of FOXP1⁺ cells in the *Vax1*^{-/-} mouse SVZ and MZ was greatly reduced at E16.5 (Fig. 4d-f', m). Striatal projection neurons were mainly composed of dopamine D1 receptor (*Drd1*) expressing MSNs and dopamine D2 receptor (*Drd2*) expressing MSNs. In situ hybridization of *Drd1-mRNA* and *Drd2-mRNA* showed that *Drd1*⁺ and *Drd2*⁺ MSNs were also reduced in *Vax1* mutant mice (Fig. 4g-l'). These results suggest striatal MSNs are decreased in *Vax1*^{-/-} mice at E16.5.

At P0, we can see a thicker SVZ in *Vax1*^{-/-} mice from the nuclear staining of DAPI (See Supplementary Fig. S2a, b, Additional File 1). The partial sequences of exon 2 and exon 3 of the *Vax1* gene were replaced by a *LacZ* reporter gene in the *Vax1*^{-/-} mice. In situ hybridization of *LacZ-mRNA* showed a marked increase of LacZ⁺ cells, suggesting that most *Vax1* mutant cells were still there (See Supplementary Fig. S2 c, d, Additional File 1). *Ki67* is expressed in dividing cells and the KI67⁺ region was the thicker LacZ⁺ SVZ

region in *Vax1*^{-/-} mice (See Supplementary Fig. S2e, f, Additional File 1), whereas, FOXP1⁺ cells were rarely detected (See Supplementary Fig. S2g-h', Additional File 1). Altogether, these results indicated the blockage of striatal MSN differentiation in the *Vax1*^{-/-} mice.

Only about 6% *Vax1*^{-/-} mice can survive to P20, and we were fortunate to have collected two P20 *Vax1*^{-/-} mouse brains. We then performed DAPI, and in situ hybridization staining of *Drd1* and *Drd2*. We observed the absence of the septum and preoptic area in the *Vax1* mutant mice, the change in the shape of the striatum, and that *Vax1* mutants had enlarged lateral ventricles (See Supplementary Fig. S3a, a', Additional File 1). The *Vax1* mutants had a low density of *Drd1*-mRNA⁺ and *Drd2*-mRNA⁺ in the medial striatum (See Supplementary Fig. S3b-c', Additional File 1). Taken together, our results showed the number of vLGE derived striatal MSNs was reduced in the *Vax1*^{-/-} mice.

3.5 The MGE domain had defects in the *Vax1*^{-/-} mice

Since the dLGE domain is enlarged and the vLGE domain is atrophic in the *Vax1*^{-/-} mice, we wanted to further investigate the change of the MGE domain in the *Vax1* mutants. We then performed in situ hybridization staining of *Nkx2.1*, *Lhx6* and *Lhx8* at E13.5. The induction and regional pattern formation of MGE are dependent on the transcription factor *Nkx2.1* [13]. *Nkx2.1* plays an important role in maintaining the specificity and differentiation of MGE progenitors [12, 32]. The *Nkx2.1*⁺ MGE domain in the *Vax1*^{-/-} mice was significantly smaller than that in the controls (Fig. 5a-c'). LIM-homeodomain transcription factors *Lhx6*, and *Lhx8*, are expressed in the MGE SVZ, and are crucial for the migration and differentiation of MGE-derived neurons. In *Vax1*^{-/-} mice, the expression of *Lhx6* and *Lhx8* was greatly reduced (Fig. 5d-i'). Thus, the interneurons in the neocortex were reduced by 30%-44% after *Vax1* gene deletion [20], possibly due to the smaller MGE domain in the *Vax1*^{-/-} mice. The progenitors in the MGE not only give rise to cortical interneurons, but also striatal interneurons and globus pallidus neurons. Many transcription factors have been found to be expressed in the globus pallidus, such as: *Nkx2.1*, *Gbx1*, *Gbx2*, *Arx*, *Dlx1*, *Etv1*, *Lhx6*, and *Lhx8* [33]. In order to know clearly the changes in the globus pallidus, we performed in situ hybridization staining of *Nkx2.1*, *Gbx1*, and *Gbx2* at E12.5 in the *Vax1*^{-/-} and control mice. We also detected *Etv1*, *Nkx2.1*, *Lhx6* and *Lhx8* at E18.5. There was a reduction in globus pallidus neurons after *Vax1* deletion (See Supplementary Fig. S4, Fig.S5, Additional File 1). In summary, the MGE domain gets smaller and MGE-derived neurons are decreased in the *Vax1*^{-/-} mice.

3.6 RNA-Seq analysis provided further molecular evidence for defects in *Vax1* mutant mice

To characterize the molecular changes in *Vax1*^{-/-} mice, we performed RNA-Seq analysis. Gene expression profiles from the embryonic day (E) 13.5 and E16.5 ganglionic eminence (GE) were analyzed. Changed expression of genes revealed by the RNA-Seq was consistent with our staining results, above. At E13.5, there was a remarkable increased expression of *Gsx2* and *Sp8* in the GE, with significantly decreased *Isl1*, *Ebf1*, *Foxp1*, *Tac1*, *Otx2*, *Lhx8*, *Gbx2*, and *Gbx1* (Table1). At E16.5, the dLGE markers (*Sp8*, *Etv1*, *Tshz1*) were up-regulated and the vLGE- derived neuronal markers (*Foxp1*, *Foxo1*, *Ikzf1*, *Ebf1*, *Gpr88*, *Tac1*, *Sox8*,

Zfp503, Drd1, Ppp1r1b, Gpr6, Isl1, Zcchc12, Adora2a) were down-regulated, with an upregulation of genes that promote cell cycle and maintenance of the progenitor state (Table2). The combined with the above staining results, compared with controls in the *Vax1*^{-/-} mice, showed that the dLGE cells invaded ventrally into the vLGE, causing the dLGE region to get larger while the vLGE and MGE regions get smaller.

3.7 Increased expression of *Gsx2* in the vLGE and MGE in *Vax1* mutant mice

Previous studies showed that *Vax1* is a fundamental regulator of ventral identity for retinal ganglion cells and *Gsx2* is a key regulator of dLGE identity for OB interneurons [4, 34-37]. In an attempt to understand the relationship between *Vax1* and *Gsx2*, we performed immunofluorescence or in situ RNA hybridization staining of *Gsx2* or *Vax1* from immediate adjacent 20 μm sections in *WT* mice at E11.5 and E16.5. We observed *Gsx2* expression as a ventral-low to dorsal-high gradient in the subpallium (Fig. 6a-c). In contrast, *Vax1* was expressed in a ventral-high to dorsal-low gradient along the subpallium (Fig. 6b-d). The expression pattern of *Vax1* is largely complementary to that of *Gsx2*, supporting our hypothesis that *Vax1* may be crucial for subpallium regionalization. To test this, we performed immunofluorescence or in situ RNA hybridization of *Gsx2* at early stages, and our results showed that the expression pattern of *Gsx2* (ventral-low to dorsal-high) was disrupted in the *Vax1*^{-/-} mice at E11.5 and E13.5 (Fig. 7a-d). *Gsx2* was highly expressed in the whole subpallium VZ and SVZ in the *Vax1*^{-/-} mice suggesting that *Vax1* may be as an inhibitor to suppress the expression of *Gsx2* in the subpallium VZ and SVZ. Altogether, these results suggest that *Vax1* may regulate subpallium regionalization by repressing *Gsx2*.

3.8 *Vax1* inhibits the expression of *Gsx2* in the progenitor cells.

To further investigate whether *Vax1* inhibits the expression of *Gsx2* during forebrain development, we over-expressed *Vax1* in the lateral neural progenitors by electroporation and analyzed the impact on *Gsx2* expression. A *Vax1* expression plasmid (pCAG-*Vax1*-GFP) or a control vector (pCAG-GFP) was electroporated into the lateral ventricular wall at P0 in the *WT* mice. Three days later, animals were sacrificed and the number of total GFP⁺ or GFP/GSX2 double positive cells was measured in the dorsal-lateral region (Fig. 8a-b). Our results showed no difference in the total number of GFP⁺ cells between control and pCAG-*Vax1*-GFP mice (Fig. 8c). However, the number of GFP/GSX2 double positive cells showed a significant decrease (5-fold) in the pCAG-*Vax1*-GFP mice compared to control mice (Fig. 8a'-b' and d). Thus, we conclude that in progenitor cells, *Vax1* has the capacity to act as a negative regulator of *Gsx2* expression.

4 Discussion

In this study, we investigated the function of the *Vax1* gene in subpallium regionalization using *Vax1*^{-/-} mice. Our results showed an increase in cell proliferation and the blockage of neuronal differentiation in the subpallium of the *Vax1*^{-/-} mice. More importantly, the dLGE expanded to the whole subpallium VZ and SVZ in the *Vax1*^{-/-} mice (Fig. 9a). We found that the *Gsx2* was highly expressed in the whole subpallium VZ and SVZ caused by *Vax1* gene deletion (Fig. 9b). Overexpression of *Vax1* in the LGE progenitors

strongly inhibits the expression of *Gsx2*. Thus, we proposed that *Vax1* may regulate the subpallium regionalization by suppressing *Gsx2* expression.

4.1 The dLGE, vLGE and MGE domain in the *Vax1-KO* mice

The full name of the *Vax1* gene is ventral anterior homeobox 1. The *Vax1* gene also is a member of the *Emx* and *Not* gene families [17]. The genes of the *Emx* and the *Not* gene families play an important role in the patterning development of the regions where they are expressed. In the *Vax1*^{-/-} mice, the progenitors in the dLGE/dSVZ domain are significantly increased, vLGE-derived striatal projection neurons are significantly decreased, MGE progenitors are decreased and the septal area is absent. This suggests that the *Vax1* gene regulates the regionalization of the subpallium. It seems that the dLGE region was significantly expanded ventrally in *Vax1*^{-/-} mice and the dLGE was enlarged at the expense of the vLGE, MGE, and septum.

The dLGE progenitors mainly give rise to OB interneurons. *Prokr2*, *Tshz1*, *Etv1*, and *Sp8* showed increased gradient expression in the dLGE/dSVZ at E16.5 and P0. Since *Gsx2* is expressed in proliferating progenitors, *Sp8* is found in some dividing cells, and *Prokr2* is observed in post-mitotic immature interneurons, this would suggest the blockage of neuronal differentiation in the dLGE after *Vax1* gene deletion. Despite the significantly increased of dLGE/dSVZ progenitors, the blockage of neuronal differentiation and defects of migration, results in *Vax1*^{-/-} mice with a severely hypoplastic OB [38].

There is a reduction of *Ebf1*⁺, *Isl1*⁺, *Foxp1*⁺, *Drd1*⁺, and *Drd2*⁺ striatal projection neurons in the striatum of *Vax1* mutant mice. Despite the increase of cell proliferation in the *Vax1*^{-/-} subpallium V-SVZ, the vLGE domain gets smaller and there is blockage of striatal MSN differentiation in the *Vax1*^{-/-} mice, this thereby, led to the developmental defects of the striatum in the *Vax1*^{-/-} mice.

MGE contributes approximately 70% of cortical interneurons and most globus pallidal projection neurons [39, 40]. The MGE domain got smaller and MGE progenitors were decreased in the *Vax1*^{-/-} mice, leading to a reduction of cortical interneurons [20] and globus pallidal neurons.

The septum is an important structure that connects many important brain structures. It begins to develop in the early embryonic stage, from E10.5 to E14.5 when septal neurons are mainly produced [41]. Progenitors in the septum not only contribute to septal neurons but also OB interneurons [37, 42]. The septum is absent in the *Vax1*^{-/-} mice suggesting that *Vax1* plays an important role in its development.

4.2 The relationship between *Vax1* and *Gsx2*

There was increased expression of *Gsx2* in the vLGE and MGE in *Vax1* mutant mice. The transcription factor *Gsx2* plays a powerful role in the development of the telencephalon [35] and is crucial for the dorsal-ventral patterning [16]. *Gsx2* and *Pax6* play important roles in the maintenance of the pallium and subpallium boundary [11, 43]. In *Gsx2* mutant mice, dLGE progenitor cells express markers of the ventral pallium (*Pax6*, *Ngn2*, *Tbr2* and *Dbx1*) during early telencephalic development. The dLGE is respecified into

a ventral pallium like structure [35, 44, 45]. *Vax1* (ventral-high, dorsal-low) and *Gsx2* (ventral-low, dorsal-high) display largely complementary patterns of expression in the developing subpallium, suggesting that *Vax1* may regulate ventral telencephalic development by repressing *Gsx2*. We performed in vivo electroporation to overexpress *Vax1* in the LGE progenitors, our results showed that *Vax1* can strongly inhibit the expression of *Gsx2*. These results suggested that *Gsx2* was down-regulated in the progenitors due to *Vax1* expression. We also performed EMSA (electrophoretic mobility shift assay) to verify whether VAX1 directly inhibits the expression of *Gsx2*. This may be due to the real motif which is not in the predicted motifs, however, we did not get a positive result.

4.3 *Gsx2* cooperated with *Pax6* and *Vax1* which are essential for telencephalic regionalization

The telencephalon is subdivided into molecularly and functionally distinct progenitor regions along the dorsal-ventral (D-V) axis that generate different subclasses of neurons. A number of developmental control genes are specifically expressed by progenitors in either the pallium or subpallium. For instance, progenitor cells in the pallium express *Emx1*, *Pax6*, and *Ngn2* [11, 46]. In the pallium, *Pax6* is critical for the progenitors' identity. The dLGE expands to the pallium in the *Pax6*^{-/-} mice as detected by dLGE markers such as *Dlx1/2*, *Sp8* and *Etv1* [47]. Progenitors in the dLGE express *Gsx2*, *Sp8*, *Etv1*, *Tshz1* and *Prokr2*. In this region, *Gsx2* is a core regulator for dLGE identity. *Gsx2* function was found to be essential to maintain the molecular identity of early striatal progenitors and in its absence the pallium regulatory genes *Pax6* and *Ngn2* are ectopically expressed in the LGE [16]. Progenitors in the MGE or POA express *Nkx2.1*, *Lhx6*, *Lhx8*, and *Otx2*. In the *Nkx2.1* mutants, the MGE gets smaller and LGE progenitors invade into the MGE primordium [13, 33]. *Otx2* was also reported to be essential for promoting vMGE identity and repressing POA identity [14]. In this study, we found that *Vax1* was highly expressed in the subpallium (dorsal-low, ventral-high). *Vax1* functions as a repressor to inhibit *Gsx2* expression for subpallium regionalization. Overall, we speculated that *Vax1*, *Gsx2*, and *Pax6* are the key regulators of the progenitors' regionalization during telencephalic development.

4.4 The increase of cell proliferation and the blockage of neuronal differentiation in the *Vax1*^{-/-} mice

In the *Vax1*^{-/-} mouse subpallium, the expression of *Gsx1* is down-regulated. *Gsx2* maintains LGE progenitors in an undifferentiated state, whereas *Gsx1* promotes progenitor maturation and the acquisition of neuronal phenotypes [48]. Therefore, that is the reason for the increase of cell proliferation and the blockage of neuronal differentiation in the *Vax1*^{-/-} subpallium.

Declarations

Acknowledgements

Not applicable.

Ethics approval and consent to participate

All experiments conducted in this research study were in accordance with guidelines from Fudan University.

Funding information

Research grants to Z. Yang. from National Key Research and Development Program of China (2018YFA0108000), National Natural Science Foundation of China (NSFC 31820103006, 31630032 and 31425011), and research grant to Y. You (NSFC 31700889).

Data availability statement

The data that support the findings of this study are available from the corresponding author upon reasonable request.

Conflict of interest statement

The authors declare that they have no competing interests.

Author contributions

All authors had full access to the data and take responsibility for the integrity of the results and the accuracy of the data analysis. Y.W., Z.Y., and Z.Z. designed the research and Y.W., Z.S., and Z.W. performed experiments and analysis. L.Y., G.L., Z.S., Y.D., H.D., Z.L., Y.Y., and X.L. helped conduct experiments. Y.W., Z.Y., and Z.Z. drafted the manuscript.

Consent for publication References

Not applicable.

References

1. Puelles, L. and J.L.R. Rubenstein, *Forebrain gene expression domains and the evolving prosomeric model*. Trends in Neurosciences, 2003. **26**(9): p. 469-476.
2. Campbell, K., *Dorsal-ventral patterning in the mammalian telencephalon*. Current Opinion in Neurobiology, 2003. **13**(1): p. 50-56.
3. Hasenpusch-Theil, K., J.A. Watson, and T. Theil, *Direct Interactions Between Gli3, Wnt8b, and Fgfs Underlie Patterning of the Dorsal Telencephalon*. Cerebral Cortex, 2017. **27**(2): p. 1137-1148.
4. Waclaw, R.R., et al., *Distinct temporal requirements for the homeobox gene Gsx2 in specifying striatal and olfactory bulb neuronal fates*. Neuron, 2009. **63**(4): p. 451-65.
5. Stenman, J., H. Toresson, and K. Campbell, *Identification of two distinct progenitor populations in the lateral ganglionic eminence: implications for striatal and olfactory bulb neurogenesis*. J Neurosci, 2003. **23**(1): p. 167-74.

6. Waclaw, R.R., et al., *The zinc finger transcription factor Sp8 regulates the generation and diversity of olfactory bulb interneurons*. *Neuron*, 2006. **49**(4): p. 503-16.
7. Gutin, G., et al., *FGF signalling generates ventral telencephalic cells independently of SHH*. *Development*, 2006. **133**(15): p. 2937-46.
8. Storm, E.E., et al., *Dose-dependent functions of Fgf8 in regulating telencephalic patterning centers*. *Development*, 2006. **133**(9): p. 1831-44.
9. Fuccillo, M., et al., *Temporal requirement for hedgehog signaling in ventral telencephalic patterning*. *Development*, 2004. **131**(20): p. 5031-40.
10. Rash, B.G. and E.A. Grove, *Patterning the dorsal telencephalon: A role for sonic hedgehog?* *Journal of Neuroscience*, 2007. **27**(43): p. 11595-11603.
11. Yun, K., S. Potter, and J.L. Rubenstein, *Gsh2 and Pax6 play complementary roles in dorsoventral patterning of the mammalian telencephalon*. *Development*, 2001. **128**(2): p. 193-205.
12. Sussel, L., et al., *Loss of Nkx2.1 homeobox gene function results in a ventral to dorsal molecular respecification within the basal telencephalon: evidence for a transformation of the pallidum into the striatum*. *Development*, 1999. **126**(15): p. 3359-70.
13. Corbin, J.G., et al., *Combinatorial function of the homeodomain proteins Nkx2.1 and Gsh2 in ventral telencephalic patterning*. *Development*, 2003. **130**(20): p. 4895-906.
14. Hoch, R.V., et al., *OTX2 Transcription Factor Controls Regional Patterning within the Medial Ganglionic Eminence and Regional Identity of the Septum*. *Cell Rep*, 2015. **12**(3): p. 482-94.
15. Chapman, H., et al., *The homeobox gene Gsx2 controls the timing of oligodendroglial fate specification in mouse lateral ganglionic eminence progenitors*. *Development*, 2013. **140**(11): p. 2289-98.
16. Toresson, H., S.S. Potter, and K. Campbell, *Genetic control of dorsal-ventral identity in the telencephalon: opposing roles for Pax6 and Gsh2*. *Development*, 2000. **127**(20): p. 4361-71.
17. Hallonet, M., et al., *Vax1, a novel homeobox-containing gene, directs development of the basal forebrain and visual system*. *Genes & Development*, 1999. **13**(23): p. 3106-3114.
18. Kim, N., et al., *Regulation of retinal axon growth by secreted Vax1 homeodomain protein*. *eLife*, 2014. **3**.
19. Soria, J.M., et al., *Defective postnatal neurogenesis and disorganization of the rostral migratory stream in absence of the Vax1 homeobox gene*. *Journal of Neuroscience*, 2004. **24**(49): p. 11171-11181.
20. Tagliabatella, P., et al., *Compromised generation of GABAergic interneurons in the brains of Vax1(-/-) mice*. *Development*, 2004. **131**(17): p. 4239-4249.
21. Coré, N., et al., *Stem cell regionalization during olfactory bulb neurogenesis depends on regulatory interactions between Vax1 and Pax6*. *eLife*, 2020. **9**.
22. Li, D., et al., *Polymorphic variants in VAX1 and the risk of nonsyndromic cleft lip with or without cleft palate in a population from northern China*. *Medicine (Baltimore)*, 2017. **96**(14): p. e6550.

23. Hoffmann, H.M., et al., *Heterozygous deletion of ventral anterior homeobox (vax1) causes subfertility in mice*. *Endocrinology*, 2014. **155**(10): p. 4043-53.
24. Wen, Y., et al., *The PROK2/PROKR2 signaling pathway is required for the migration of most olfactory bulb interneurons*. *J Comp Neurol*, 2019.
25. Zhang, Z., et al., *Zfhx3 is required for the differentiation of late born D1-type medium spiny neurons*. *Exp Neurol*, 2019: p. 113055.
26. Liu, Z., et al., *Sp9 Regulates Medial Ganglionic Eminence-Derived Cortical Interneuron Development*. *Cerebral Cortex*, 2018.
27. Horton, S., et al., *Correct coordination of neuronal differentiation events in ventral forebrain requires the bHLH factor MASH1*. *Mol Cell Neurosci*, 1999. **14**(4-5): p. 355-69.
28. Li, J., et al., *Transcription Factors Sp8 and Sp9 Coordinately Regulate Olfactory Bulb Interneuron Development*. *Cereb Cortex*, 2017: p. 1-17.
29. Prosser, H.M., A. Bradley, and M.A. Caldwell, *Olfactory bulb hypoplasia in Prokr2 null mice stems from defective neuronal progenitor migration and differentiation*. *Eur J Neurosci*, 2007. **26**(12): p. 3339-44.
30. Ehrman, L.A., et al., *The LIM homeobox gene Isl1 is required for the correct development of the striatonigral pathway in the mouse*. *Proc Natl Acad Sci U S A*, 2013. **110**(42): p. E4026-35.
31. Lu, K.M., et al., *Dual role for Islet-1 in promoting striatonigral and repressing striatopallidal genetic programs to specify striatonigral cell identity*. *Proc Natl Acad Sci U S A*, 2014. **111**(1): p. E168-77.
32. Sandberg, M., et al., *Transcriptional Networks Controlled by NKX2-1 in the Development of Forebrain GABAergic Neurons*. *Neuron*, 2016. **91**(6): p. 1260-1275.
33. Flandin, P., S. Kimura, and J.L. Rubenstein, *The progenitor zone of the ventral medial ganglionic eminence requires Nkx2-1 to generate most of the globus pallidus but few neocortical interneurons*. *J Neurosci*, 2010. **30**(8): p. 2812-23.
34. Schulte, D., et al., *Misexpression of the Emx-related homeobox genes cVax and mVax2 ventralizes the retina and perturbs the retinotectal map*. *Neuron*, 1999. **24**(3): p. 541-553.
35. Corbin, J.G., et al., *The Gsh2 homeodomain gene controls multiple aspects of telencephalic development*. *Development*, 2000. **127**(23): p. 5007-20.
36. Lopez-Juarez, A., et al., *Gsx2 controls region-specific activation of neural stem cells and injury-induced neurogenesis in the adult subventricular zone*. *Genes Dev*, 2013. **27**(11): p. 1272-87.
37. Qin, S., et al., *Septal contributions to olfactory bulb interneuron diversity in the embryonic mouse telencephalon: role of the homeobox gene Gsx2*. *Neural Dev*, 2017. **12**(1): p. 13.
38. Soria, J.M., *Defective Postnatal Neurogenesis and Disorganization of the Rostral Migratory Stream in Absence of the Vax1 Homeobox Gene*. *Journal of Neuroscience*, 2004. **24**(49): p. 11171-11181.
39. Kessar, N., et al., *Genetic programs controlling cortical interneuron fate*. *Curr Opin Neurobiol*, 2014. **26**: p. 79-87.

40. Hu, J.S., et al., *Cortical interneuron development: a tale of time and space*. Development, 2017. **144**(21): p. 3867-3878.
41. Wei, B., et al., *The onion skin-like organization of the septum arises from multiple embryonic origins to form multiple adult neuronal fates*. Neuroscience, 2012. **222**: p. 110-123.
42. Inoue, T., et al., *Zic1 and Zic3 regulate medial forebrain development through expansion of neuronal progenitors*. J Neurosci, 2007. **27**(20): p. 5461-73.
43. Desmaris, E., et al., *DMRT5, DMRT3, and EMX2 Cooperatively Repress Gsx2 at the Pallium-Subpallium Boundary to Maintain Cortical Identity in Dorsal Telencephalic Progenitors*. J Neurosci, 2018. **38**(42): p. 9105-9121.
44. Toresson, H. and K. Campbell, *A role for Gsh1 in the developing striatum and olfactory bulb of Gsh2 mutant mice*. Development, 2001. **128**(23): p. 4769-80.
45. Wang, B., et al., *Ascl1 is a required downstream effector of Gsx gene function in the embryonic mouse telencephalon*. Neural Dev, 2009. **4**: p. 5.
46. Puelles, L., et al., *Pallial and subpallial derivatives in the embryonic chick and mouse telencephalon, traced by the expression of the genes Dlx-2, Emx-1, Nkx-2.1, Pax-6, and Tbr-1*. J Comp Neurol, 2000. **424**(3): p. 409-38.
47. Guo, T., et al., *Dlx1/2 are Central and Essential Components in the Transcriptional Code for Generating Olfactory Bulb Interneurons*. Cereb Cortex, 2019.
48. Pei, Z., et al., *Homeobox genes Gsx1 and Gsx2 differentially regulate telencephalic progenitor maturation*. Proceedings of the National Academy of Sciences, 2011. **108**(4): p. 1675-1680.

Tables

Table1: The significantly changed gene at E13.5

Gene Name	Vax1 ^{-/-} (FPKM)	WT(FPKM)	P-value	Gene Name	Vax1 ^{-/-} (FPKM)	WT(FPKM)	P-value
<i>Gsx2</i>	23.14	13.38	1.14E-05	<i>Sp8</i>	14.54	9.97	0.000109
<i>Bmp2</i>	0.33	0.15	0.019487	<i>Gsx1</i>	1.35	3.34	1.60E-07
<i>Wnt8b</i>	0.26	0.01	0.000507	<i>Olig2</i>	24.76	33.79	0.009027
<i>Col2a1</i>	9.47	3.43	1.03E-08	<i>Lhx8</i>	7.22	18.93	7.45E-08
<i>Rpl21</i>	9.39	3.54	9.74E-06	<i>Gbx2</i>	1.54	3.56	2.27E-05
<i>Pcdhga9</i>	9.16	1.67	2.00E-06	<i>Gbx1</i>	4.07	8.90	5.27E-08
<i>Zfp125</i>	6.61	2.51	0.018824	<i>Isl1</i>	13.07	19.52	0.000176
<i>Pcdhgb5</i>	5.09	1.22	0.003204	<i>Ebf1</i>	9.35	13.38	0.000134
<i>Zbtb9</i>	5.05	0.75	0.000337	<i>Pcdhgb8</i>	0.60	14.38	3.11E-07

Table2: The significantly changed gene at E16.5

Gene Name	<i>Vax1</i> ^{-/-} (FPKM)	WT(FPKM)	P-value	Gene Name	<i>Vax1</i> ^{-/-} (FPKM)	WT(FPKM)	P-value
<i>Gsx2</i>	48.57	21.93	6.51E-20	<i>Ikzf1</i>	5.13	95.76	4.1E-194
<i>Sp8</i>	129.05	40.62	3.97E-64	<i>Ebf1</i>	19.71	279.67	3.4E-186
<i>Etv1</i>	121.40	68.67	1.12E-11	<i>Gpr88</i>	40.54	157.96	1.2E-128
<i>Tshz1</i>	218.54	124.77	1.77E-34	<i>Foxp1</i>	136.78	509.22	1.6E-128
<i>Id2</i>	8.60	2.79	1.02E-13	<i>Foxo1</i>	11.09	72.42	1.1E-110
<i>Btg2</i>	71.76	53.39	1.31E-06	<i>Tac1</i>	1.56	30.79	9.2E-119
<i>Cdk1</i>	88.43	59.89	3.04E-08	<i>Sox8</i>	65.38	169.49	1.21E-97
<i>Cdk6</i>	103.61	63.07	0.000564	<i>Aldh1a3</i>	0.71	24.35	1.05E-83
<i>Cdk17</i>	183.13	114.80	4.78E-17	<i>Zfp503</i>	51.52	165.63	8.52E-66
<i>Cdk2</i>	63.56	45.21	9.82E-07	<i>Drd1</i>	2.29	16.78	7.88E-44
<i>Cdk2ap1</i>	184.03	118.16	2.69E-32	<i>Ppp1r1b</i>	4.07	19.33	4.32E-39
<i>Cdca7</i>	442.29	233.64	7.27E-32	<i>Gpr6</i>	0.51	2.58	5.01E-09
<i>Hes5</i>	43.41	29.83	2.17E-05	<i>Isl1</i>	13.88	212.04	1.8E-150
<i>E2f1</i>	59.81	31.77	9.53E-20	<i>Zcchc12</i>	23.66	154.32	1.2E-140
<i>Rnd3</i>	355.58	234.16	1.07E-18	<i>Adra2a</i>	1.06	6.39	1.47E-24
<i>Ube2ql1</i>	193.94	117.69	4.57E-35	<i>Pdyn</i>	0.55	4.13	5.49E-18
<i>Smo</i>	108.05	63.65	1.41E-27	<i>Zfp521</i>	18.90	90.34	1.7E-125
<i>Gli3</i>	117.85	55.41	1.62E-27	<i>Cadm1</i>	64.43	193.31	9.8E-122
<i>Gli2</i>	59.45	38.33	7.8E-08	<i>Syt4</i>	13.74	177.66	8.5E-302
<i>Fgf3</i>	9.48	4.97	6.73E-07	<i>Plk2</i>	39.49	228.74	2.1E-268
<i>Wnt5a</i>	52.20	14.95	1.87E-43	<i>Rarb</i>	8.12	109.08	2.4E-236
<i>Tgif2</i>	86.59	36.18	5.74E-48	<i>Nrxn1</i>	35.01	165.06	2.5E-222
<i>Grik3</i>	492.09	340.76	2.28E-08	<i>Cdh13</i>	7.57	43.06	2.49E-73
<i>Slit1</i>	208.78	126.45	9.4E-37	<i>Cdh8</i>	14.27	115.01	6.2E-174
<i>ErbB4</i>	184.81	142.53	4.59E-06	<i>Rph3a</i>	18.23	120.03	1.9E-165
<i>Tcf4</i>	771.87	374.27	2.59E-22	<i>Tgfa</i>	9.71	52.16	9.81E-55
<i>Atp5e</i>	63.64	1.61	1.7E-230	<i>Gsx1</i>	1.68	6.11	5.46E-15
<i>Ppp1r14b</i>	189.02	103.54	1.35E-47	<i>Nkx2-1</i>	14.10	63.19	5.18E-14
<i>Sox5</i>	78.28	36.11	3.3E-34	<i>Gbx2</i>	0.03	0.81	1.1E-07
<i>Ascl1</i>	211.46	142.65	4.75E-12	<i>Gbx1</i>	0.23	1.70	1.82E-05
<i>Dlx1</i>	1405.97	735.12	1.02E-09	<i>Olig1</i>	7.37	16.12	5.66E-07
<i>Sp9</i>	457.87	279.05	4.37E-16	<i>Sox10</i>	0.76	3.08	8.77E-06
<i>Nr2f2</i>	38.23	12.90	2.32E-33	<i>Calb1</i>	4.39	24.55	4.76E-33
<i>Arx</i>	399.99	310.76	3.42E-06	<i>Npy</i>	4.79	20.62	3.69E-39
<i>Pbx1</i>	582.92	418.62	4.01E-06	<i>Sst</i>	2.66	15.65	2.86E-28
<i>Cux1</i>	321.52	260.59	1.66E-05	<i>Cxcl14</i>	2.76	6.37	1.38E-07
<i>Htr3a</i>	17.76	3.92	4.92E-28	<i>Robo1</i>	136.64	295.71	7.08E-60
<i>Prox1</i>	115.39	41.09	1.22E-48	<i>Reln</i>	11.53	108.95	5E-178

Figures

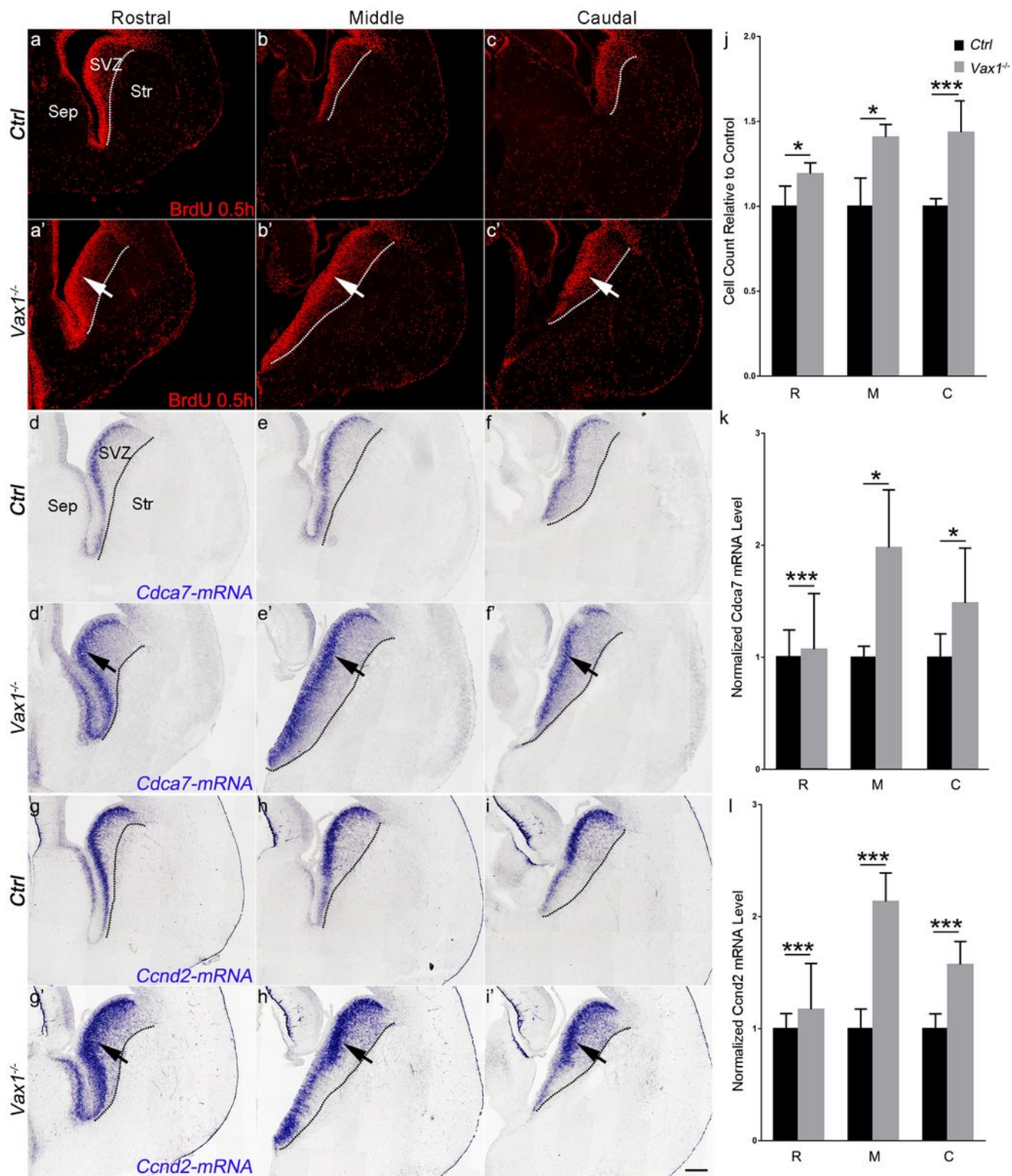


Figure 1

Increase of cell proliferation in the Vax1^{-/-} subpallium V-SVZ at E16.5. (a-c') A single injection of BrdU was administered into mice at E16.5 and BrdU immunostaining was analyzed 30-minutes later. Immunofluorescence staining of BrdU showed that BrdU⁺ cells were significantly increased in the Vax1^{-/-} subpallium V-SVZ. (d-i') In situ hybridization showed that Cdca7-mRNA⁺ and Ccnd2-mRNA⁺ cells were also significantly increased in the Vax1^{-/-} subpallium. (j-l) Histograms show quantification data of BrdU,

Cdca7 and Ccnd2. (Student's t-test, * $P < .05$, *** $P < .001$, $n=3$ mice per group, mean \pm SEM). Arrows indicate the number of BrdU, Cdca7 and Ccnd2 is increased. Abbreviations: Sep (septum), SVZ (subventricular zone), Str (Striatum), R (rostral), M (middle) and C (Caudal). Scale bars: 200 μ m in i' for a-i'.

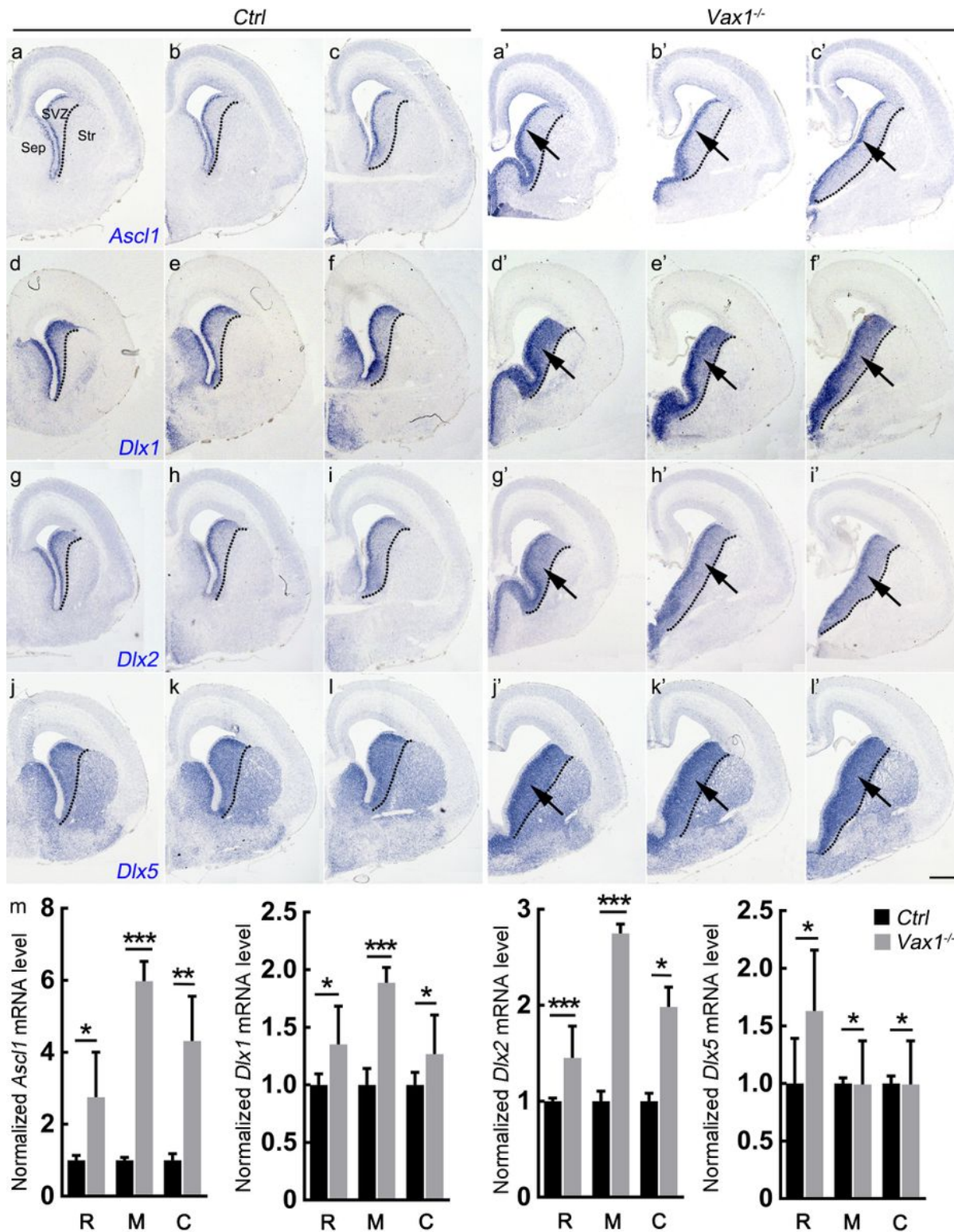


Figure 2

Neural progenitor cells accumulate in the subpallium V-SVZ of *Vax1*^{-/-} mice. (a-l') In situ hybridization of *Ascl1*, *Dlx1*, *Dlx2* and *Dlx5* in the E16.5 *Vax1*^{-/-} subpallium. *Ascl1*⁺, *Dlx1*⁺, *Dlx2*⁺, and *Dlx5*⁺ cells in the *Vax1*-KO subpallium were markedly increased. (m) The quantification data showed that the expression of the *Ascl1*, *Dlx1*, *Dlx2* and *Dlx5* was increased in the LGE SVZ of *Vax1*-KO mice. (Student's t-test, **P* < .05, ***P* < .01, ****P* < .001, *n*=3 mice per group, mean ± SEM). Scale bars: 500 μm in l' for a-l'.

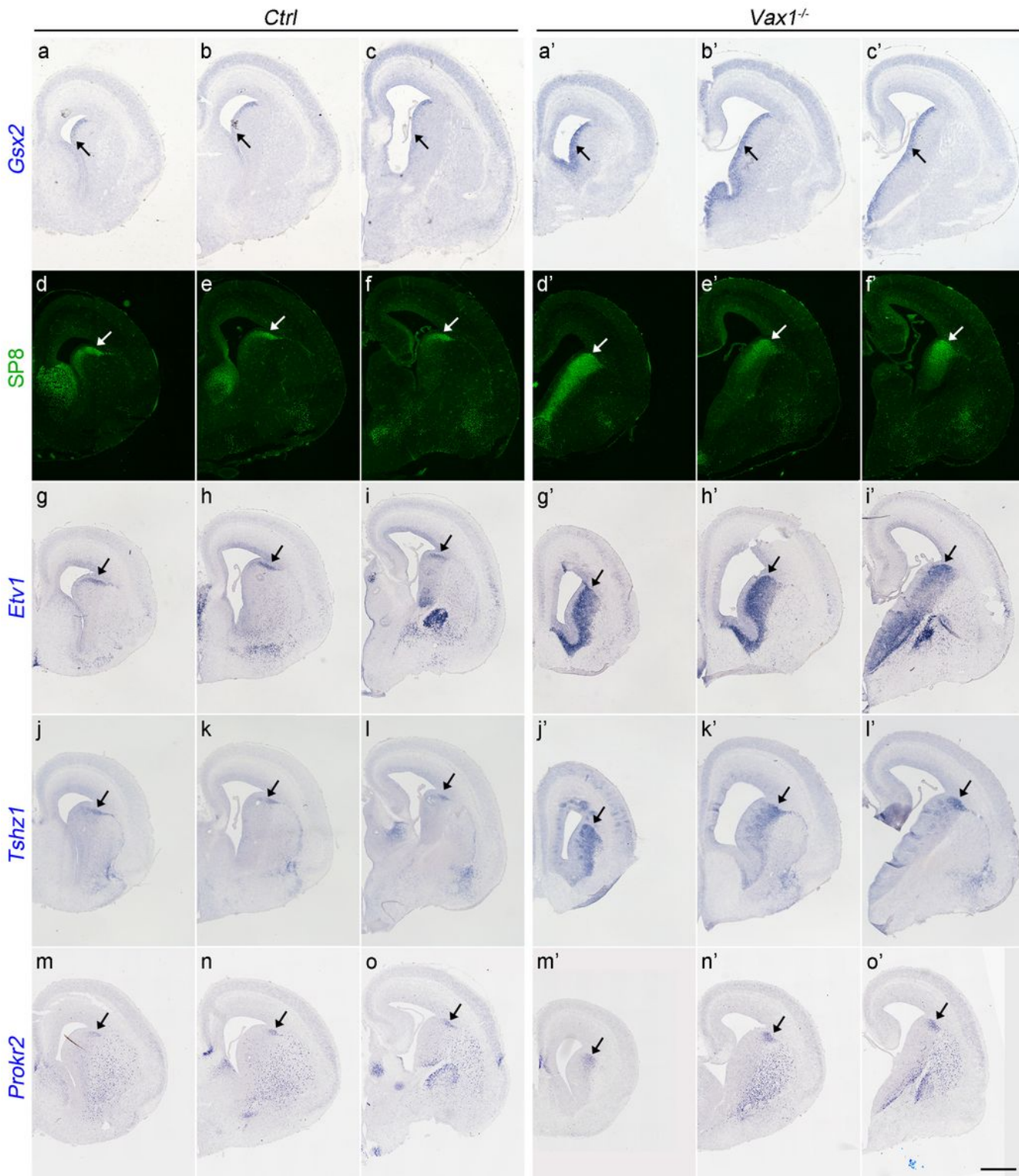


Figure 3

Increased expression of *Gsx2*, *Sp8*, *Etv1*, *Tshz1* and *Prokr2* in the E16.5 *Vax1*^{-/-} mice. (a-c') In situ hybridization of *Gsx2* showed increased expression of *Gsx2* in the vLGE in *Vax1* mutant mice. (d-f') SP8 immunostaining showed that the number of SP8⁺ cells in the *Vax1*^{-/-} mouse dLGE was significantly increased at E16.5. (g-o') *Etv1*⁺, *Tshz1*⁺, and *Prokr2*⁺ cells in the *Vax1*^{-/-} mouse dLGE were also increased. N = 3 mice per group. Scale bars: 500 μ m in o' for a-o'.

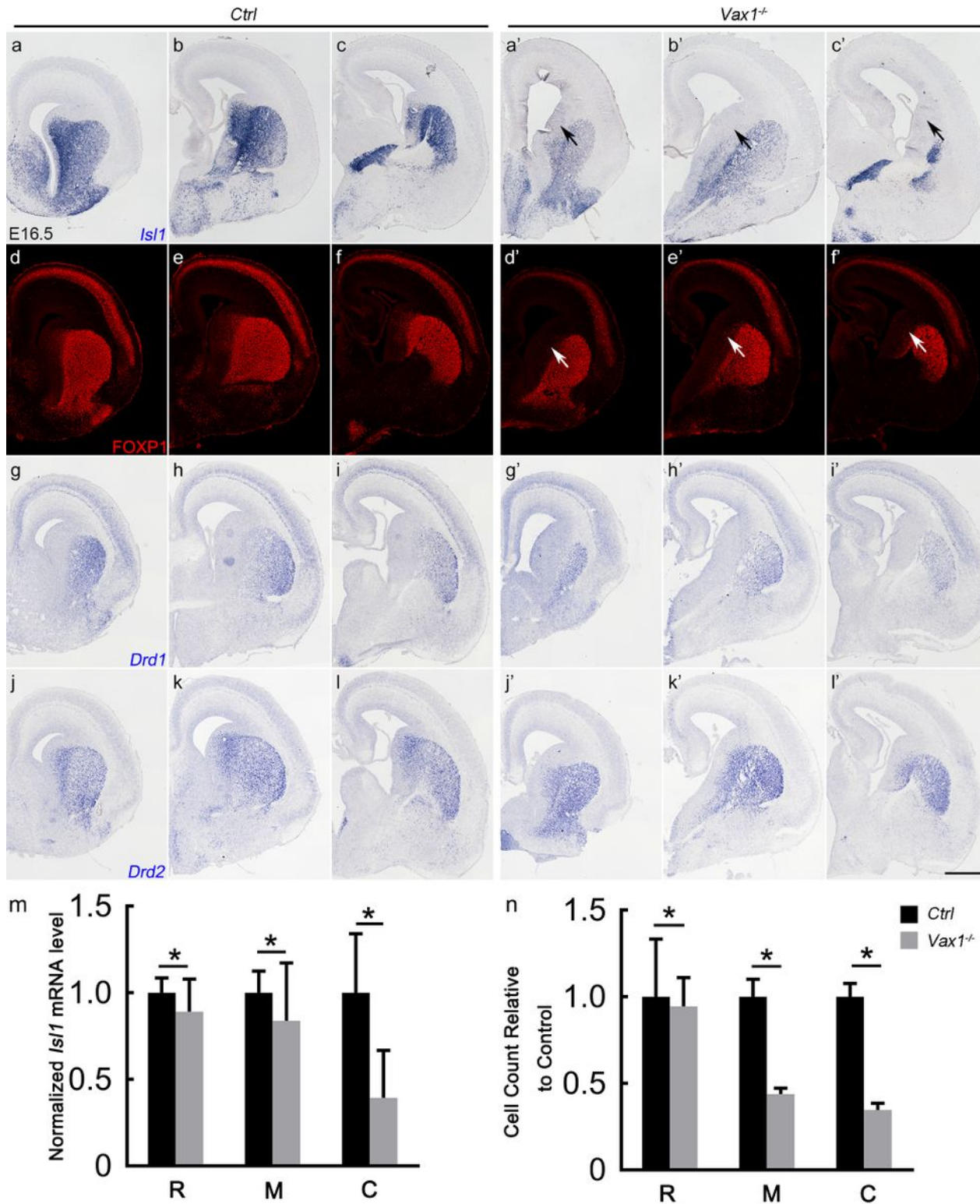


Figure 4

The vLGE-derived striatal MSNs were disrupted in *Vax1*-KO mice at E16.5. (a-c') In situ hybridization of *Isl1* at E16.5 showed *Isl1*-mRNA+ cells in the vLGE SVZ were significantly decreased (arrows). (d-f') Immunofluorescence staining showed that the *FOXP1*+ cells in LGE SVZ were greatly reduced (arrows) at E16.5. (g-i') In situ hybridization of *Drd1* and *Drd2* showed *Drd1*+ and *Drd2*+ MSNs were reduced in *Vax1* mutant mice. (m-n) Quantification data showed that the expression of *Isl1* and *Foxp1* was reduced in the LGE SVZ from rostral to caudal. (Student's t-test, * $P < .05$, $n=3$ mice per group, mean \pm SEM). Scale bars: 500 μ m in l' for a-l'.

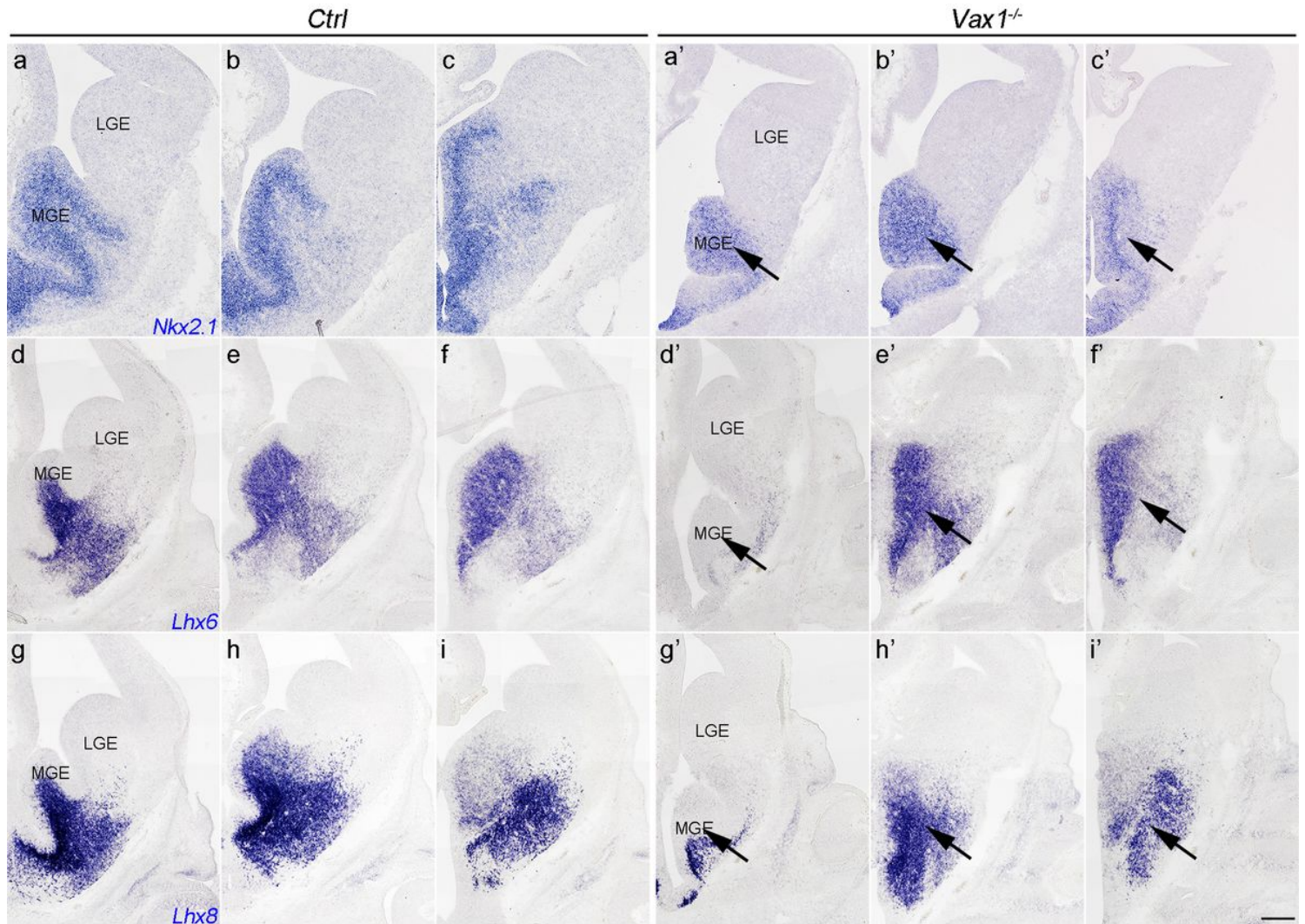


Figure 5

The MGE domain gets smaller in the *Vax1*-KO mice at E13.5. (a-i') In situ RNA hybridization staining for *Nkx2.1*, *Lhx6* and *Lhx8* at E13.5. The *Nkx2.1*+ domain in the *Vax1*^{-/-} mice was smaller than that in the controls and the expression of *Lhx6* and *Lhx8* was greatly reduced in the MGE of *Vax1* mutants. Arrows indicate the expression of *Nkx2.1*, *Lhx6* and *Lhx8* is decreased. $N = 3$ mice per group. Scale bars: 200 μ m in i' for a-i'.

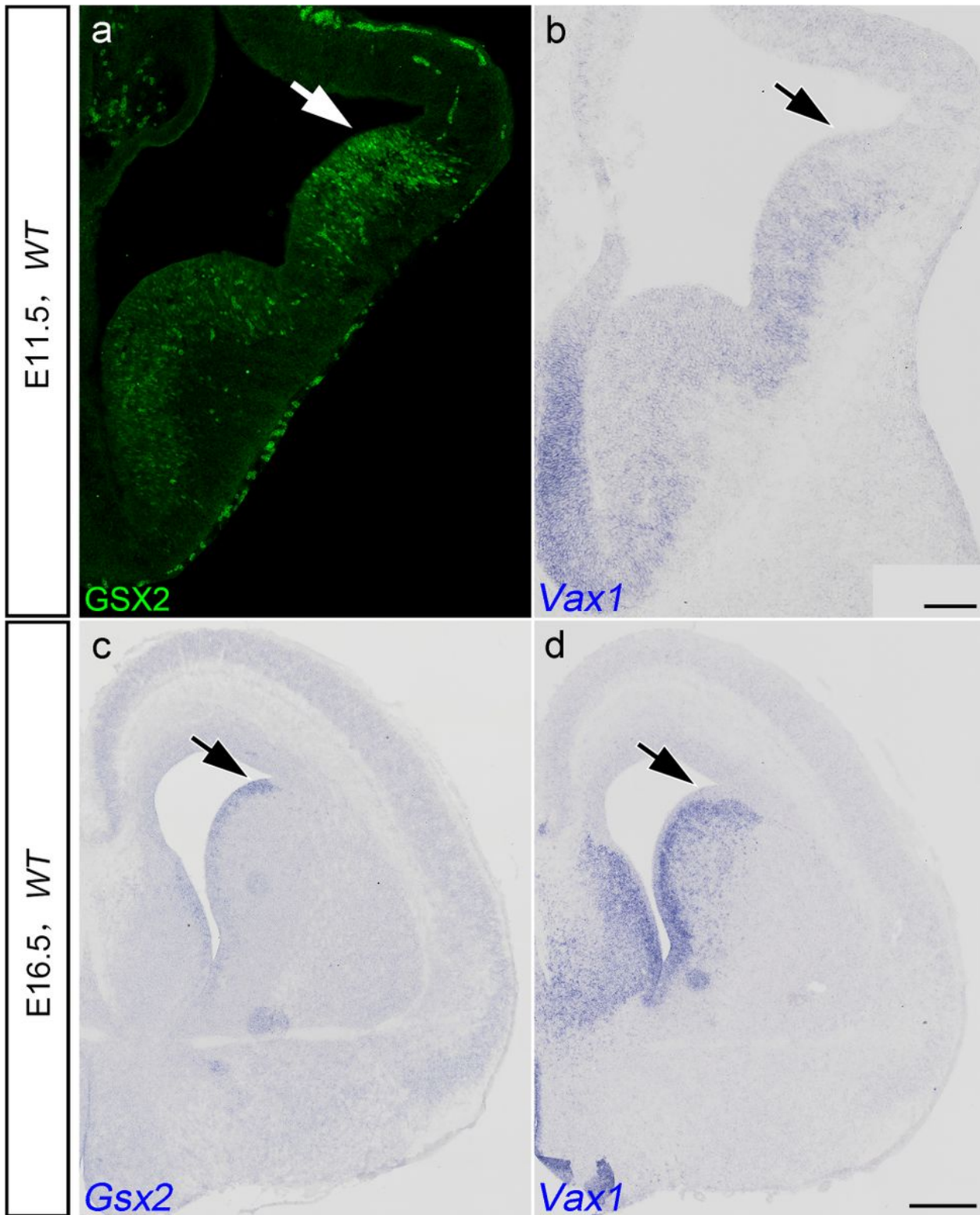


Figure 6

Complementary expression of Vax1 and Gsx2 in the subpallium. (a, b) Immunofluorescence staining of Gsx2 and in situ RNA hybridization staining of Vax1 from immediately adjacent 20- μ m sections in WT mice at E11.5. Gsx2 was strongly expressed in the dLGE and the expression of Vax1 in this region was weak. (c, d) In situ RNA hybridization staining of Gsx2 and Vax1 from immediately adjacent 20- μ m

sections in WT mice at E16.5; Vax1 and Gsx2 display largely complementary patterns of expression in the subpallium. N = 3 mice per group. Scale bars: 200 μ m in b for a-b, 500 μ m in d for c-d.

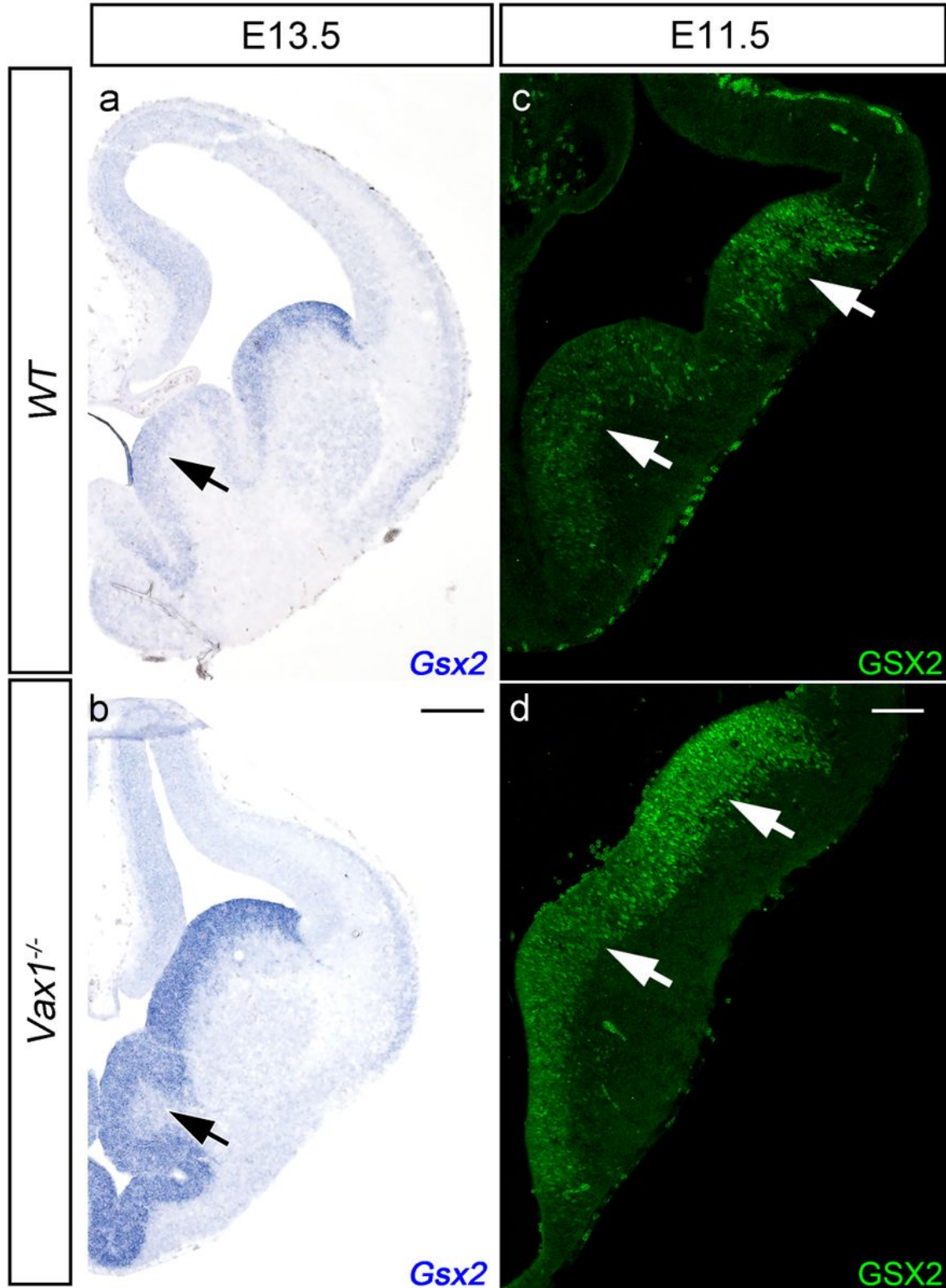


Figure 7

Increased expression of Gsx2 in the vLGE and MGE in Vax1 mutant mice. (a, b) The Gsx2⁺ cells were seen in the VZ of the vLGE and MGE and there was no longer an obvious ventral to dorsal gradient of the Gsx2 expression pattern in the Vax1^{-/-} mice. (c, d) Immunofluorescence staining of GSX2 at E11.5. There

was increased expression of Gsx2 in the vLGE and MGE in the Vax1 mutant mice. N = 3 mice per group. Scale bars: 500 μ m in b for a-b, 200 μ m in d for c-d.

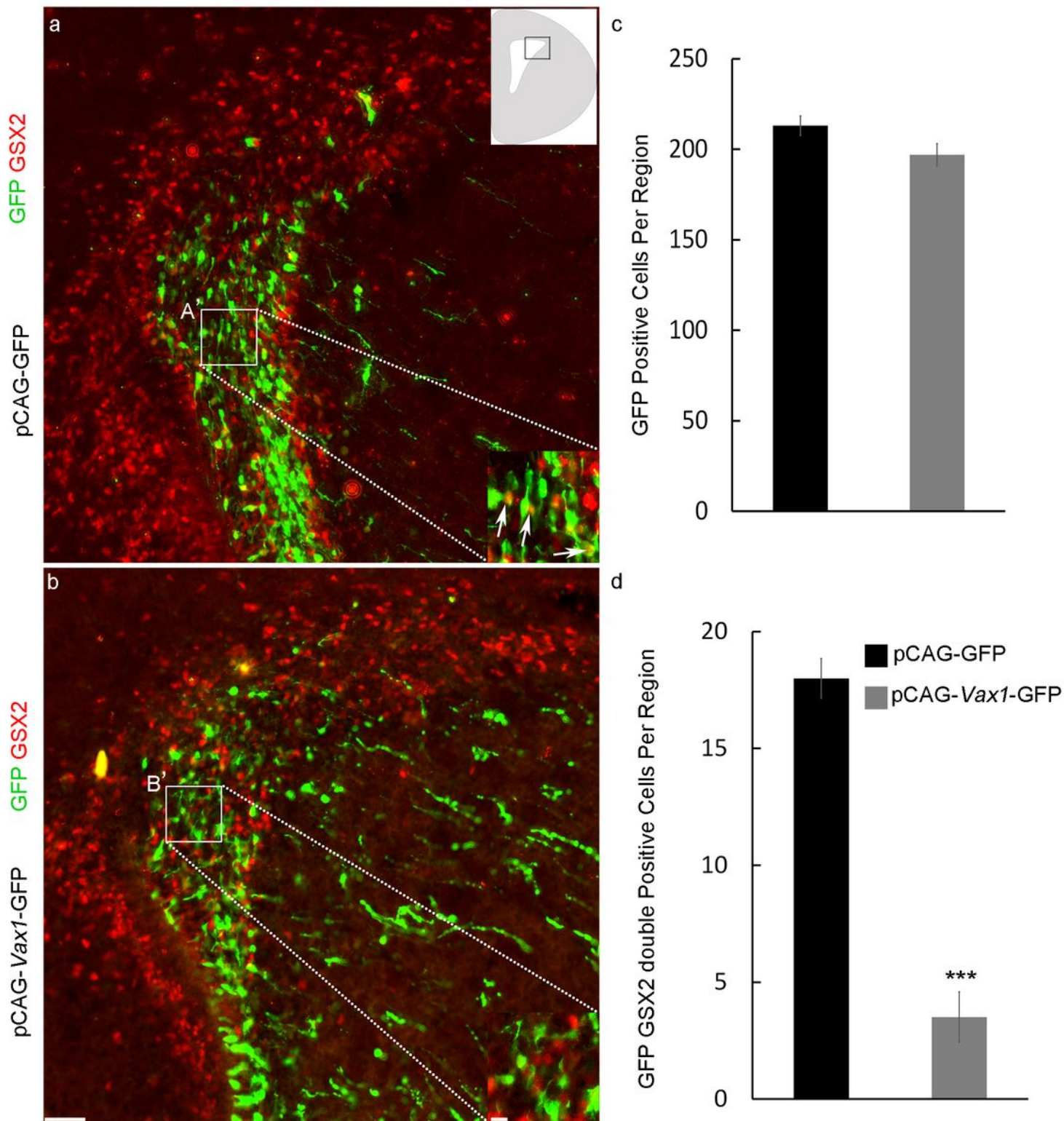


Figure 8

The expression of Gsx2 was suppressed by Vax1 in progenitor cells. (a) Many GSX2+ cells were co-labelled with GFP+ cells in control mice. (b) Very few GSX2 /GFP double positive cells were observed in Vax1 over-expressing mice. (c) Quantification of GFP+ cells in control or Vax1 over-expressing mice. (d)

Quantification GFP /GSX2 double positive cells in control or Vax1 over-expressing mice. (a', b') High-magnification images illustrating the downregulation of GSX2 in GFP+ cells after electroporation of the lateral V-SVZ by Vax1. White arrows: GFP / GSX2 double positive cells. Student's t-test, ***P < .0001, n=5 mice per group, mean \pm SEM. N = 5 mice per group. Scale bars: 50 μ m in b for a-b, 20 μ m in b' for a'-b'.

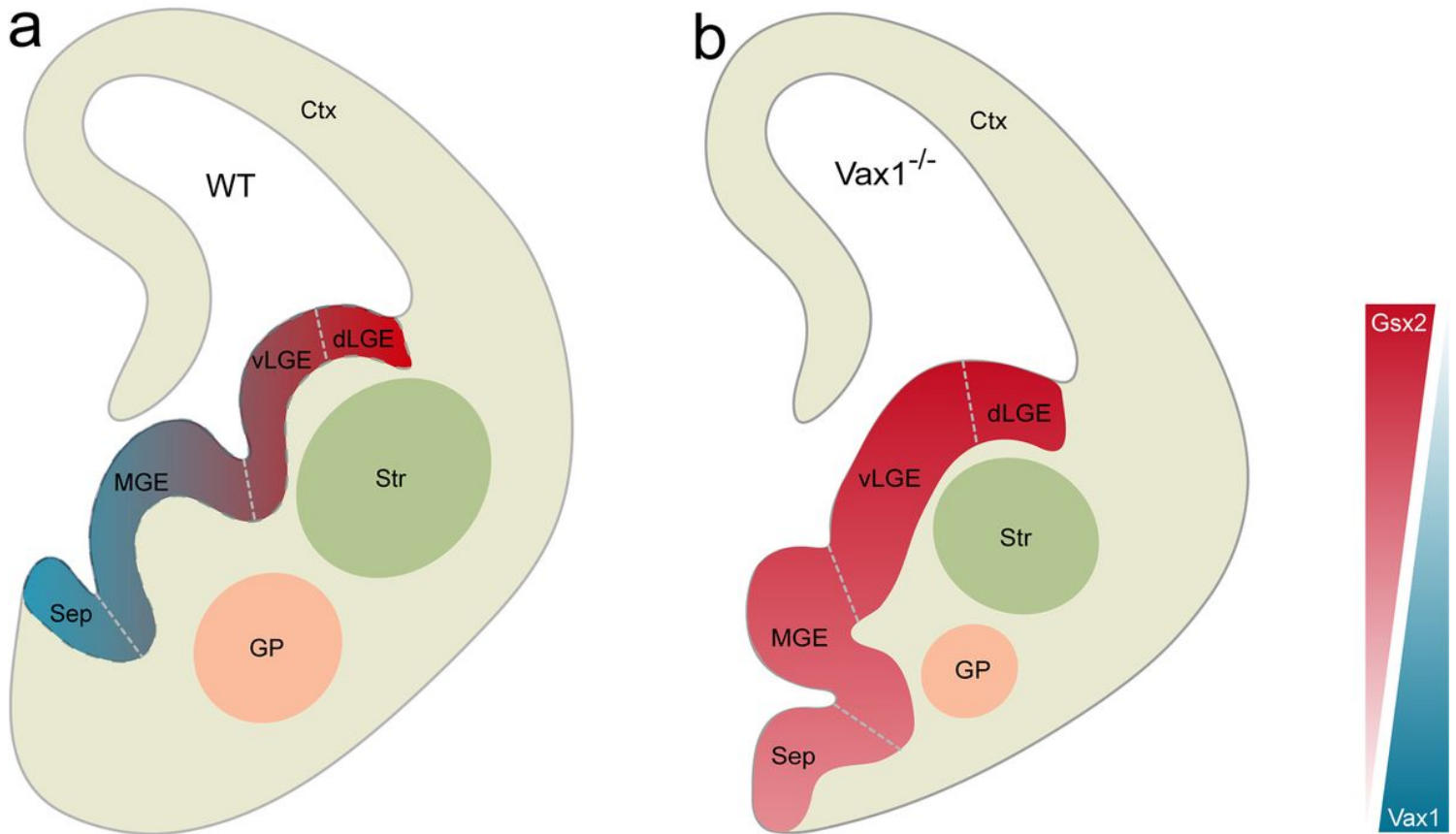


Figure 9

A model of Vax1 regulates subpallium regionalization. (a) The expression patterns of Vax1 and Gsx2 are largely complementary. Gsx2 expressed in a ventral-low to dorsal-high gradient while the Vax1 was expressed in a ventral-high to dorsal-low gradient along the subpallium. (b) Increased expression of Gsx2 in the vLGE and MGE leads to the abnormal cell proliferation and differentiation of the subpallium neurons in Vax1 mutant mice.

Supplementary Files

This is a list of supplementary files associated with this preprint. Click to download.

- [AdditionalFile1.pdf](#)